smart cities

MDPI

Article

An Integrated Climate-Resilient Prototype for Year-Round Outdoor Workout Equipment

Pauls P. Argalis [1,*], Maris Slezins [2] and Aleksandrs Ivasko [3]

[1] Institute of Sustainable Building Materials and Engineering Systems, Faculty of Civil and Mechanical Engineering, Riga Technical University, Kipsalas Str. 6A, LV-1048 Riga, Latvia
[2] Ltd. "Kenguru Pro", Lauteres Street 4, LV-1002 Riga, Latvia
[3] Ltd. "Aimconcept", Satekles Street 2C, LV-1050 Riga, Latvia
* Correspondence: pauls-pavils.argalis@rtu.lv

Highlights

What are the main findings?

- In staged outdoor scenarios, an on-site vision-language model recognised falls, loss of grip, slipping and prolonged immobility, and generated structured alerts for the person in charge.
- A motion-analysis model trained on participants with different body proportions reached a keypoint mean average precision of 0.906 and counted repetitions in real time.

What are the implications of the main findings?

- Sharing one power supply, backup, network connection and enclosure among surveillance, exercise feedback, and heating removes duplicated hardware.
- Combining on-site AI analysis, human alert verification, and a heated grip zone provides a basis for safer, year-round outdoor workout parks.

Abstract

Public outdoor workout facilities are used less in winter and are not monitored for safety, and deploying individual smart technologies separately duplicates hardware and creates structural clutter. This study aims to design an integrated, climate-resilient outdoor workout prototype that combines AI-based safety surveillance, markerless exercise feedback and a heated grip zone on a shared power and data infrastructure, and to evaluate its surveillance and motion-analysis subsystems. The surveillance subsystem, based on an on-site vision-language model, was tested in staged outdoor scenarios, and the motion-analysis model was trained on video of participants with different body proportions and exercise techniques. In these scenarios, the system recognised falls, loss of grip, slipping, and prolonged immobility; assigned a risk level that accounted for visible weather and surface conditions; and generated structured alerts for the person in charge. The motion-analysis model achieved a keypoint mean average precision of 0.906 on the validation set, counted repetitions, and flagged incorrectly executed movements in real time. The heated grip zone uses a self-regulating cable controlled by the bar surface temperature. The results indicate that the subsystems can be combined into one asset, making outdoor workout equipment safer and usable year-round.

Academic Editor: Javier Prieto

Received: 6 October 2026
Revised: 17 November 2026
Accepted: 24 November 2026
Published: 27 November 2026

Copyright: © 2026 by the authors. Licensee MDPI, Basel, Switzerland. This article is an open access article distributed under the terms and conditions of the Creative Commons Attribution (CC BY) license.

Keywords: outdoor workout equipment; vision-language model; pose estimation; video surveillance; smart city

1. Introduction

Outdoor workout equipment supports the World Health Organisation target of 150 min of moderate-to-vigorous physical activity per week [1]. Outdoor callisthenics parks provide accessible bodyweight resistance training for diverse groups [2] without recurring user costs [3], but their value depends on safe conditions, structural integrity and year-round use [4].

Installing fitness zones in parks has been shown to increase park users' physical activity [5]. Observed use is, however, often short, with about 12 users per hour at peak times and less than 9 min per visit in one park [6], and video-based observation in another park showed that adults used the equipment as intended about 77% of the time and youth only about 39% [7]. This indicates a need for guidance on correct exercise execution at the equipment.

In temperate and cold climates, outdoor exercise declines in winter because precipitation and cold weather discourage outdoor activity [8]. Steel bars, with high thermal conductivity ($k \sim 45$ W/(m·K)), quickly cool to ambient temperature and rapidly extract heat from skin on contact [9]. Ice on the bar makes grip unpredictable because ice friction depends strongly on temperature, sliding speed and surface roughness [10]. People wear gloves, but this changes grip and can cause injuries [11].

Outdoor workout equipment also operates without human oversight or automated safety monitoring. However, injuries are common among street workout practitioners: 62.4% of 93 surveyed practitioners reported an injury in the previous 12 months, most often in the shoulder and back [12]. Injuries have been linked to overuse and to specific skills, including lumbar extension-based movements, and some pull-up variants increase glenohumeral rotation and the risk of shoulder impingement [13]; without feedback, such loads remain uncorrected. In severe acute trauma, the absence of monitoring leaves emergency assistance dependent on bystanders [14].

Outdoor fitness installations and the technologies added to them are also subject to standards and regulations. EN 16630 specifies safety requirements and test methods for permanently installed outdoor fitness equipment [15], and EN 1177 specifies impact-attenuating surfacing and how to determine critical fall height [16]. ISO 13732-3 provides methods for assessing human responses to contact with cold surfaces [17], which is relevant to metal grips in winter. Video monitoring of public spaces processes personal data. It must comply with the General Data Protection Regulation [18]. The EU Artificial Intelligence Act prohibits, with narrow exceptions, the use of real-time remote biometric identification systems in publicly accessible spaces for law enforcement [19]. These requirements determine how safety monitoring and exercise feedback can be added to outdoor equipment.

Deep-learning video management systems (VMS) provide continuous monitoring of public spaces, including in low light [20,21]. Deep anomaly detectors trained on real-world surveillance video lower the false-alarm rate compared with reconstruction-based detectors (1.9 compared with 27.2 in a real-world benchmark) [22]. Vision-language models have more recently been used as feature extractors for video anomaly detection [23]. Edge-deployed platforms can thus support automated public-safety monitoring [24].

Markerless pose estimation extracts up to 33 skeletal keypoints from a single RGB camera in real time. It measures joint angles with reported differences from marker-based reference systems of 2.6–11° for flexion–extension and abduction–adduction [25]. It runs

https://doi.org/10.3390/smartcities9120207

at more than 30 frames per second on a mobile phone [26] and can segment repetition phases and assess posture without wearable sensors [27]. On-device repetition counting has been demonstrated on a smartphone [28]. This enables real-time exercise form feedback [29].

Self-regulating conductive heating elements are used to heat pipelines and floor and ceiling structures and to prevent ice accretion [30]. When applied to a metal bar, this heating keeps the grip surface above freezing. Electrothermal heating with controlled power distribution prevents ice accretion on exposed surfaces [31].

These systems require a reliable power and data backbone: edge computing processes energy and sensor data near the source [32], and 4G/5G cellular gateways connect edge platforms to remote management systems [33] in smart cities [34].

However, these systems remain fragmented: surveillance serves crime deterrence, pose estimation is used mainly indoors, and heating is found only in passive public seating [35]. Sensor-based activity monitoring has been tested in community workout parks [36] and interactive smart floors in public settings [37], but each addresses a single function. No framework integrates AI safety monitoring, exercise feedback and heating in one installation. Separate computers, power supplies and modems for each function duplicate hardware, whereas shared edge computing can improve energy management [38].

This study therefore aims (i) to design an integrated, climate-resilient outdoor workout prototype that combines AI-based safety surveillance, markerless exercise feedback and a heated grip zone on a shared power and data infrastructure; (ii) to evaluate the surveillance subsystem in staged outdoor scenarios; (iii) to train and evaluate the motion-analysis model; and (iv) to define the integration logic through which the subsystems exchange data.

The main contributions of this study are threefold: (1) an integrated design in which AI video surveillance, markerless exercise feedback and a heated grip zone share one power, data and enclosure infrastructure; (2) a risk assessment that combines visual detection with weather and surface conditions and with the bar temperature; and (3) privacy-oriented processing, in which video is analysed on site without identity or facial recognition, and alerts are verified by a person in charge.

2. Methodology

The research design utilised a modular approach to construct and evaluate three subsystem prototypes: a modern security surveillance system, a digital interactive training enhancement system and a heated comfort structure, which are combined in one outdoor installation. The development phases included drafting technical specifications, selecting components, designing the software architecture, and evaluating the subsystems in staged outdoor scenarios. The research procedure is shown in Figure 1.

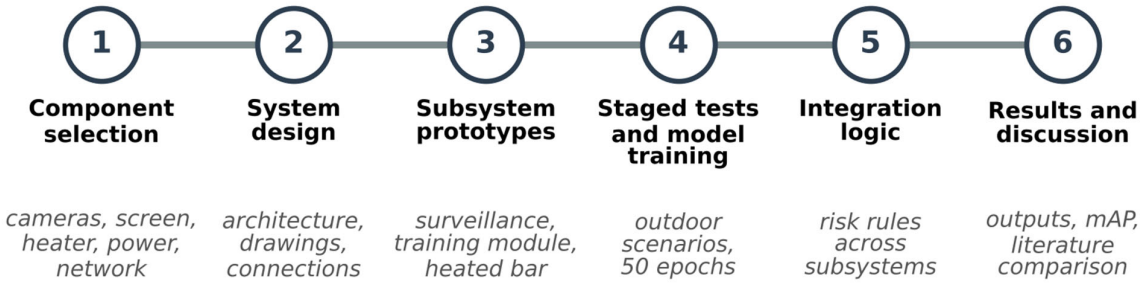


Figure 1. Research procedure of the study.

2.1. Power and Connectivity Architecture

Operating electronics outdoors requires a resilient power and data backbone. The installation is grid-connected: the 230 V supply is routed through a Victron Energy Phoenix 24/1200 inverter and an APC Smart-UPS SMT1500IC (1500 VA/1000 W), which bridges short supply interruptions. A 370 W LONGi solar panel (LR4-60HPH-370M) with an MPPT charge controller supplements battery charging and reduces grid load. A Teltonika RUTX50 4G/5G router handles high-speed data exchange across all onboard sensors and processing units. Figure 2 shows the prototype's power supply and heating connections.

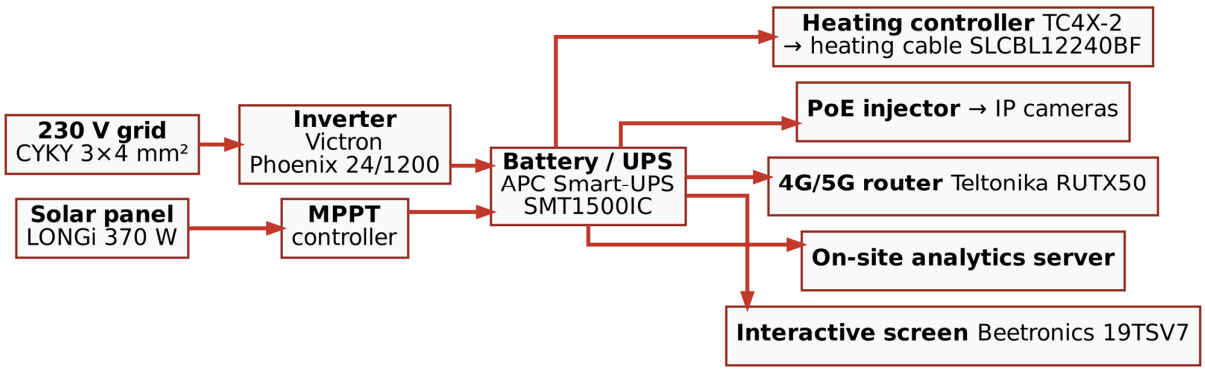


Figure 2. Prototype power supply and heating connections. The inverter, UPS, heating controller, PoE injector and router are housed in the IP66 distribution cabinet.

2.2. Intelligent Security Surveillance

Hikvision DS-2CD2347G2-L (4MP ColorVu, AcuSense) IP cameras drive site security and automated monitoring, delivering high-resolution video even in low-light outdoor conditions. The system processes feeds locally through a centralised Luxriot VMS configured with custom security rules. When the system detects a potential incident, it processes the video on site and alerts the person in charge, who assesses the situation and decides on the response; the AI does not contact security or emergency services directly. The layout of the video camera pole is shown in Figure A1 (Appendix A).

The data connections between the cameras, the on-site analytics server, the interactive screen, the bar sensors and the person in charge are shown in Figure 3.

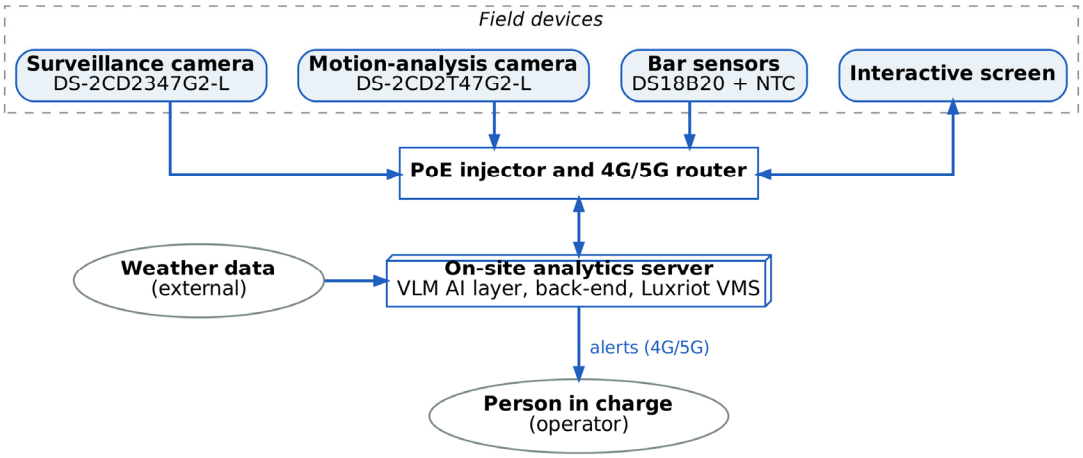


Figure 3. Data flow between the prototype subsystems.

The system architecture developed provides for the integration of several technological layers:

- Acquisition of video surveillance data from IP cameras;
- Processing and analysis of video streams on the central analytics server;
- The use of artificial intelligence algorithms for object recognition and behavioural analysis;
- Automated event classification and alarm generation;
- Data logging and statistical analysis.

The AI layer was developed by Aimconcept and runs on the on-site analytics server, so that the video is processed at the edge. It consists of a front end for configuration and review; a back end that stores configurations, analysis scenarios, and event history; and a vision-language model (VLM) that analyses video frames. The model is configured through structured instructions that define the tasks, object categories, activity types, situation classes, risk levels, and output format. Each situation is assigned one of three risk levels: normal activity, activity requiring attention and activity requiring an immediate response from the person in charge. Alarms in the Luxriot VMS are generated from probes, which are pairs of positive and negative text descriptions of a situation, and the scores of both descriptions and the margin between them are stored with each alarm. When an operator corrects a misclassified situation, the system stores the correction and can use it to train the model further.

This system module continuously processes video streams and performs real-time frame analysis. The artificial intelligence model receives the video signal from the camera, divides it into consecutive frames, and, in each frame, identifies visible objects, determines their location, classifies them, and analyses their movement.

During the initial processing stage, the system reads the video stream's technical parameters, including the camera source, frame rate, resolution, connection status, and processing time. The AI model then identifies people, workout equipment and other objects, assigning them temporary tracking identifiers.

The system determines the number of people and their location on the pitch, their position relative to sports equipment, movement direction, speed, and trajectory. Using body pose analysis, the system determines the positions of key body points and joints, enabling recognition of exercises, hanging from a bar, dynamic movements, falls, slips, loss of grip, or prolonged immobility.

The AI model also analyses interactions between people, physical contact, potential conflicts, suspicious behaviour and the inappropriate use of sports equipment. In addition, it can identify visual characteristics of clothing, such as clothing type and predominant colours, without performing personal identity or facial recognition.

At the same time, the system assesses the surrounding environment—surface condition, visible obstacles, lighting levels, precipitation, and other conditions identifiable within the video frame. Visual analysis can be supplemented with external weather data, such as temperature, rain, snow, wind speed and humidity.

The system combines weather information with video analysis results to determine the risk level more accurately. For example, a person standing on a high pole in the rain or on wet equipment is assessed as high risk. Similarly, a fall onto a wet, icy or hard surface can automatically increase the severity of an incident.

The system recognises various activities, such as pull-ups, hanging from a bar, strength exercises, dynamic elements, jumps, controlled landings, loss of grip, slipping, or falling. The AI analyses not only individual frames but also the entire sequence of movements to understand how the situation develops over time.

For example, the system can determine that a person approached the pull-up bar, began the exercise, performed a dynamic movement, lost their grip and fell. After the fall,

https://doi.org/10.3390/smartcities9120207

the AI continues to monitor the person to determine whether they got up, remained lying down, moved unsteadily or showed signs of possible injury.

For each identified object, the system generates a structured data set which may include the object type, its coordinates within the frame, a tracking identifier, the recognition confidence level, the detected activity, movement status, location zone and risk level. Events are also tagged with a start time, duration and end time.

The video analysis results are sent to the back-end system in a structured format. The back end processes the received data, stores the event history, and combines results from several consecutive frames into a single description of the situation or incident. Thus, the system does not display each frame as a separate event; instead, it creates a clear sequence of actions.

If the AI detects a potentially dangerous incident, it generates an alert message containing structured information about the situation. The message may specify the detected activity, the area of the sports ground, the equipment type, the weather conditions, the surface condition, the risk level, and the recommended response.

As a result, the user receives not only a video feed via the front-end interface, but also structured, real-time analytics on people, their activities, the sports equipment they use, environmental conditions, and potential safety risks. The system helps to determine whether the current situation constitutes normal activity, requires further attention, or calls for an immediate response from the person in charge.

2.3. AI-Powered Motion Analysis

To deliver personalised workout guidance, the station includes an industrial Beetronics 19TSV7 touchscreen. Positioned alongside it, a specialised Hikvision DS-2CD2T47G2-L IP camera captures movement in real time. Using a pose-estimation and exercise-analysis model trained by Aimconcept for this application, the system tracks joint angles, estimates body pose and identifies exercise phases without storing personal biometric data. A custom front-end and back-end server architecture processes incoming video streams, runs trained AI models, and displays instant visual and text-based form corrections directly on the screen.

The motion-analysis pipeline is shown in Figure 4. Camera frames are processed on the device at 30 frames per second. For each frame, the pose model estimates 17–33 body keypoints, which are normalised by scaling to torso length and centring on the hips, so the analysis does not depend on the user's height, body proportions, or distance from the camera. From the normalised keypoints, the system extracts the features relevant to each exercise; for the pull-up, these are the elbow flexion angle, the position of the hands relative to the shoulders, the vertical displacement of the body, the position of the head and chin relative to the hands and the bar, and the movement of the hips and knees. A repetition state machine follows the movement through the hang, pull, top, and lower phases, and counts a repetition only when the full sequence is complete. Form validators then count, flag or reject each repetition; to suppress false counts caused by small body movements or image jitter, a position must be held for a minimum time, and the movement must meet the criteria defined for the exercise. The model was trained on video of participants of different heights, body masses, and exercise techniques who performed the same exercises correctly and incorrectly.

The computer vision pipeline processed image frames strictly in RAM at the edge, extracting numeric vector coordinates without saving, recording, or transmitting raw facial or biometric video data.

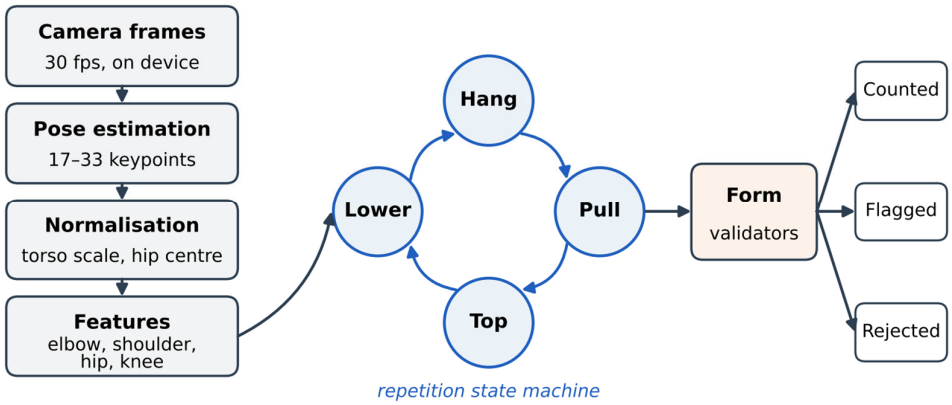


Figure 4. Motion-analysis pipeline: keypoint processing, repetition state machine and form validation.

2.4. Heated Comfort Systems

To keep the equipment usable in cold weather, a self-regulating heating cable (BriskHeat SLCBL12240BF) is installed inside the steel pull-up bar along its grip zone (Figure 5). The cable has a nominal output of 39 W/m at 10 °C for a 240 V supply; its output rises as the cable cools and falls as it warms, limiting the surface temperature without external control, and its maximum maintenance temperature is 65 °C [39]. Along the 1.87 m bar, this corresponds to about 70 W at 10 °C. The cable enters the bar through Ø 20 mm holes and is connected through a JBM050 junction box at the top of the post. The supply cable runs inside the post and underground, at a depth of 200 mm, to the IP66 distribution cabinet that houses the inverter, UPS, and heating controller. The bar is mounted 2600 mm high on posts set 700 mm into concrete foundations.

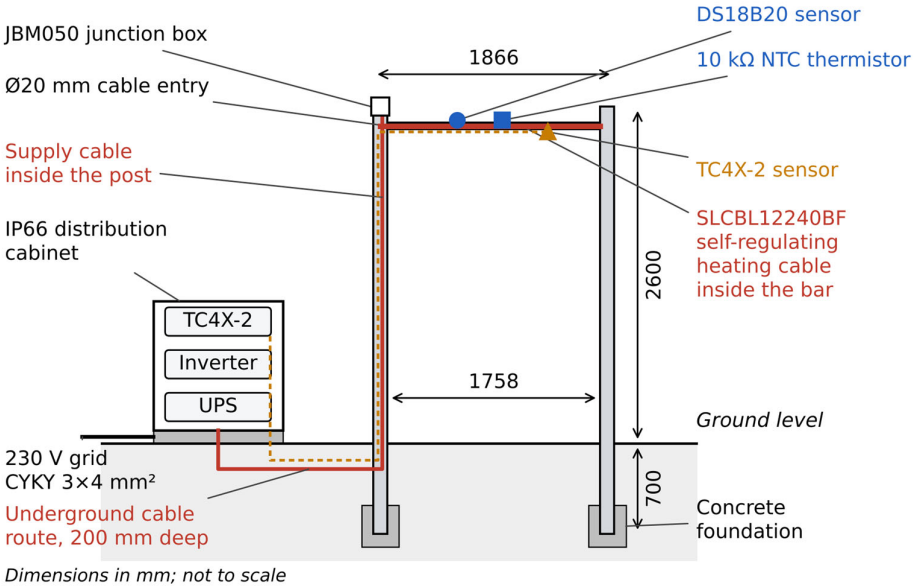


Figure 5. Layout of the heated pull-up bar and its power supply, based on the design drawing (dimensions in mm, not to scale).

Heating is switched by a TC4X-2 digital temperature controller with its sensor on the bar surface. The controller provides on/off control from −34 to 100 °C, with ±1 °C accuracy between −15 and 75 °C, and switches loads up to 10 A at 240 V [40]. It energises the cable

when the bar surface temperature falls below the set point; the target grip surface temperature is +5 to +10 °C. A DS18B20 digital sensor and a 10 kΩ NTC thermistor placed in the heated zone send the bar surface temperature to the central back end, which uses it in the risk assessment and shows the thermal readiness of the bar on the interactive screen ; the NTC thermistor provides a redundant reading for safety monitoring.

2.5. System Interaction

The individual modules interact through a central back-end processing unit. The central system combines motion tracking, equipment status, and live weather data gathered from surveillance cameras—such as active rainfall or snow. By continually evaluating user motion against environmental factors like icy or wet surfaces, the AI calculates risk levels in real time. If the system detects a hazardous condition or a fall, it instantly warns the user on the interactive screen and sends an alert across the Luxriot surveillance network. The proposed prototype design is shown in Figure 6.

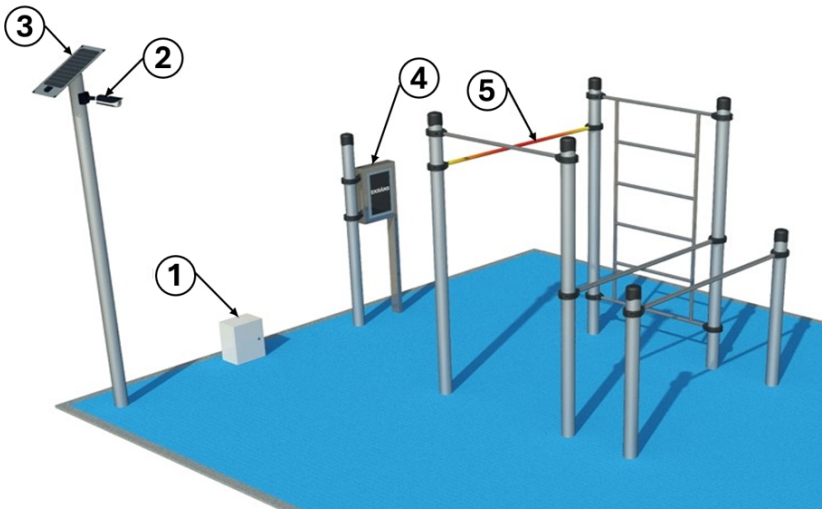


Figure 6. Proposed prototype design: (1) IP66 distribution cabinet; (2) surveillance camera; (3) solar panel; (4) interactive screen with the motion-analysis camera; and (5) heated pull-up bar.

2.6. Evaluation Approach and Data Sources

The evaluation combined three types of evidence, which are kept separate in the following sections. The surveillance subsystem was tested on installed outdoor workout equipment in staged scenarios in which participants performed normal exercise, falls from the bar, loss of grip, slipping, and prolonged immobility; for each scenario, the detected objects, activity labels, assigned risk level, and generated alert were checked. The motion-analysis model was trained on videos of participants with different heights, body mass, body proportions, and exercise techniques, who performed the same exercises both correctly and incorrectly, so the model could learn both forms of execution. All participants appearing in the video recordings gave their consent. Quantitative values describing the hardware and the class of algorithms used, such as low-light camera sensitivity, network latency, pose-estimation speed and accuracy, false-alarm rates, heating cable output and cold-contact temperature thresholds, are taken from the peer-reviewed literature and standards and, where no published value exists for the specific device, from the manufacturer's documentation; each value is cited where it is used. The alert dispatch time and the grip surface temperature range are design targets of the prototype. Training of the motion-analysis model was monitored using training and validation loss, and keypoint mean average precision (mAP) on the validation set.

2.7. Privacy and Data Protection

Data protection was designed in line with the General Data Protection Regulation (GDPR). Video is processed on site. Because the system does not identify individuals, it does not use remote biometric identification, which the EU Artificial Intelligence Act restricts in publicly accessible spaces [19]. The surveillance AI does not perform identity or facial recognition, and the motion-analysis module processes frames in device memory without recording or transmitting video. Access to video and alarm data in the Luxriot VMS is controlled through user roles and access rights; user actions are logged, and data are encrypted during transmission. Alerts are shown to the person in charge, who verifies the situation before any response, and only the information needed for the response is passed on.

3. Results

This section presents the results of the staged surveillance scenarios, the training and use of the motion-analysis model, and the prototype's integration logic.

3.1. Surveillance and Incident Detection Staged Surveillance Scenarios

The security surveillance system, powered by Hikvision DS-2CD2347G2-L (4MP ColorVu, AcuSense) IP cameras mounted on the structural mast (Component 2, Figure 6), was tested in staged scenarios on the installed equipment, in daylight and in wet weather. In these scenarios, the system recognised pull-ups, hanging from the bar, dynamic elements, loss of grip, slipping, falls and prolonged immobility, and generated structured alerts for the person in charge; the alert chain is designed to deliver a notification within 2 s of event detection.

Figures 7–11 show the surveillance subsystem output in these scenarios. For each analysed sequence, the VLM produced a scene description, an activity description and points to note; in the example in Figure 7, it described the wet paving and advised caution for activities involving footing or equipment stability.

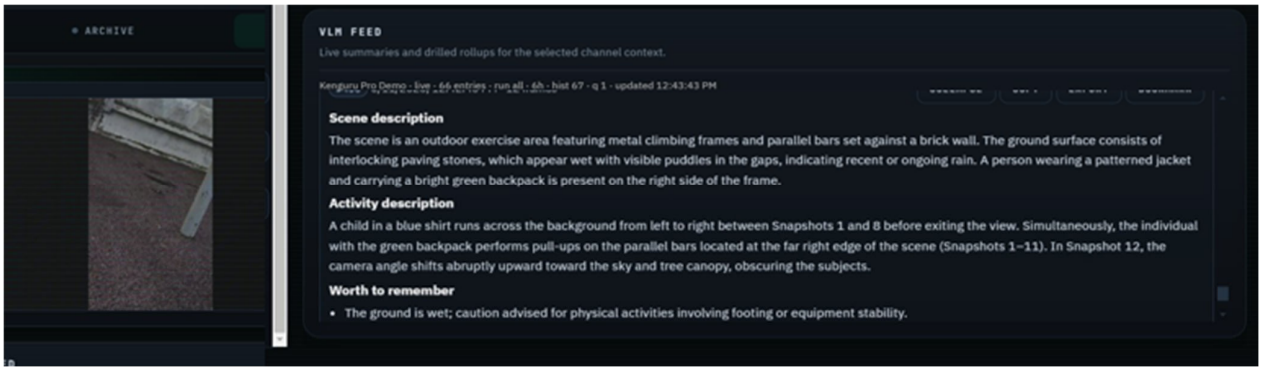


Figure 7. AI analysis of the video feed.

The AI agent also answered operator queries about archived events. In reply to a query about the same camera, it reported that the ground had been wet throughout the day and that a person had performed several pull-ups at about 11:45, and concluded that pull-ups had been done while the ground was wet (Figure 8).

The back end combined consecutive frames into one description of the action sequence and issued a structured alert, here 'Pull-up Exercise on Wet Bar' with the severity information (Figure 9).

In the Luxriot VMS, the detections appeared as alarms with their probe labels while the person exercised (Figure 10).

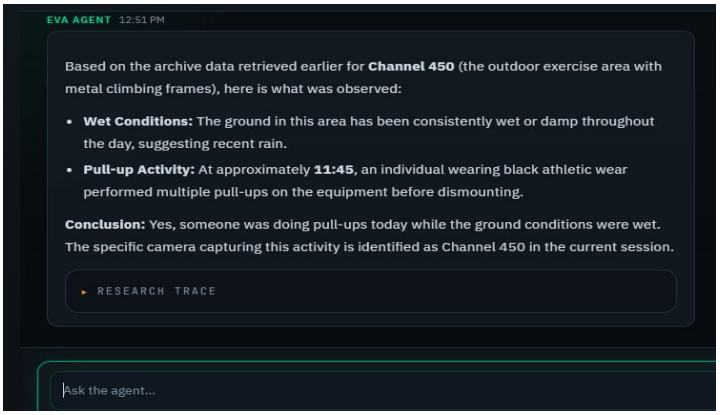


Figure 8. Summary of an AI agent's analysis of the video feed.

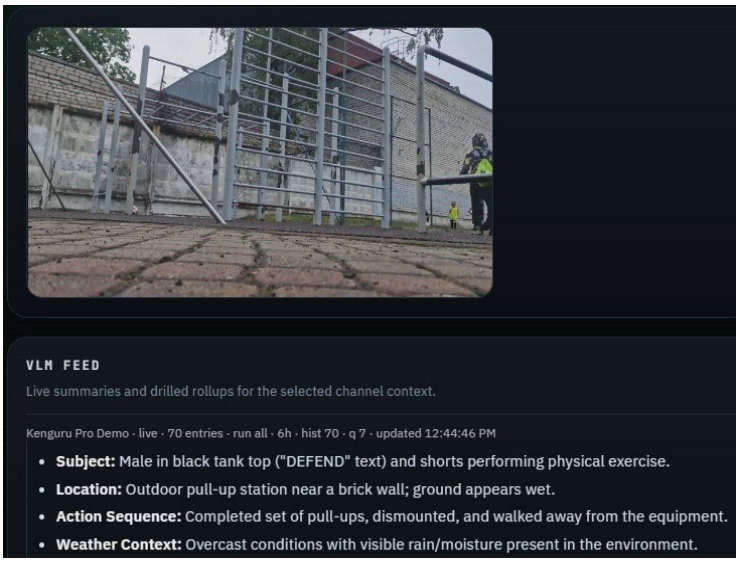


Figure 9. Sequence of actions summary in the chat log.

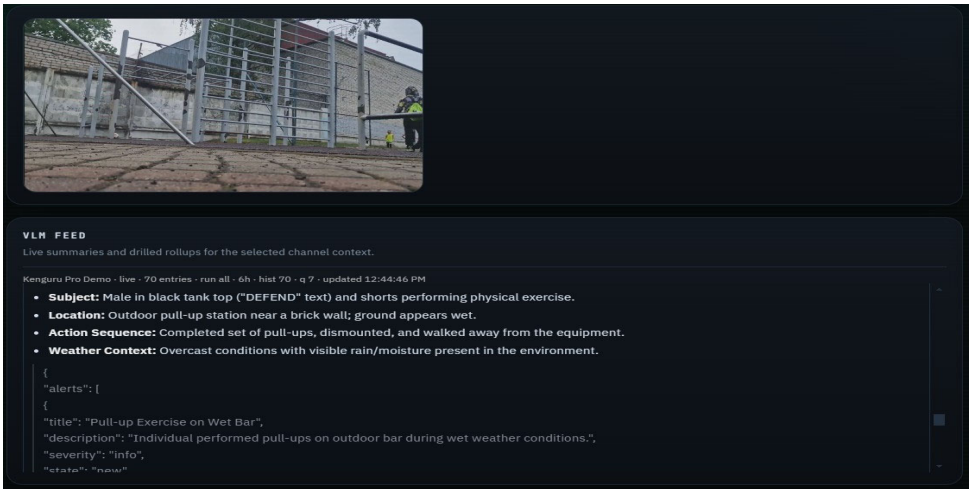


Figure 10. AI reaction to people training.

Figure 11 shows the record of an alarm raised for a dangerous workout event, with the severity 'High' and probe scores of 0.312 for the positive and 0.202 for the negative description (margin 0.111).

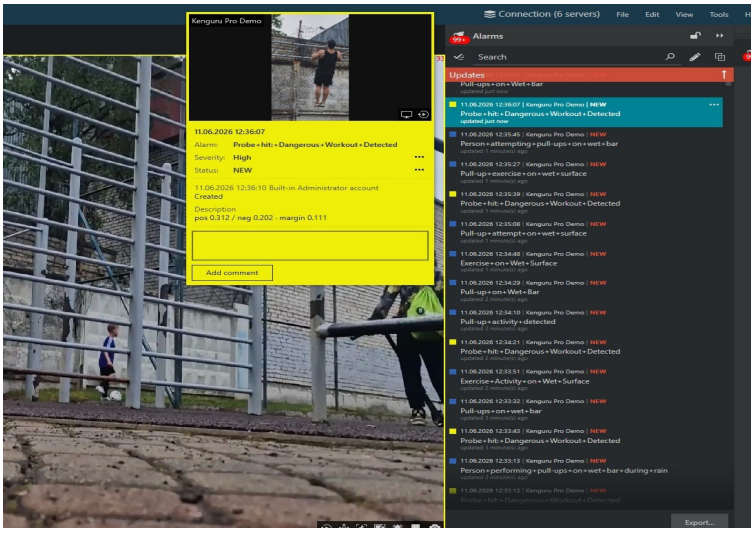


Figure 11. Example of real-life observation.

3.2. Motion Analysis Motion-Analysis Model Training and Interface

The interactive training module integrates the specialised Hikvision DS-2CD2T47G2-L camera and the Beetronics 19TSV7 industrial touchscreen interface (Component 4, Figure 6) to perform markerless human pose estimation during outdoor workouts with the motion-analysis model described in Section 2.3.

The software segmented each repetition into the hang, pull, top and lower phases and flagged repetitions that did not meet the form criteria. Real-time visual overlays and on-screen text prompts guided exercise correction.

The motion-analysis model was trained for 50 epochs (Figure 12). The training loss decreased from 0.0823 after the first epoch to 0.0103 after the last, and the validation loss decreased from 0.0714 to 0.0098. The keypoint mAP on the validation set rose from 0.512 after the first epoch to 0.736 after 10 epochs, 0.865 after 30 epochs and 0.906 after 50 epochs. The validation loss remained slightly below the training loss throughout training, which shows no sign of overfitting.

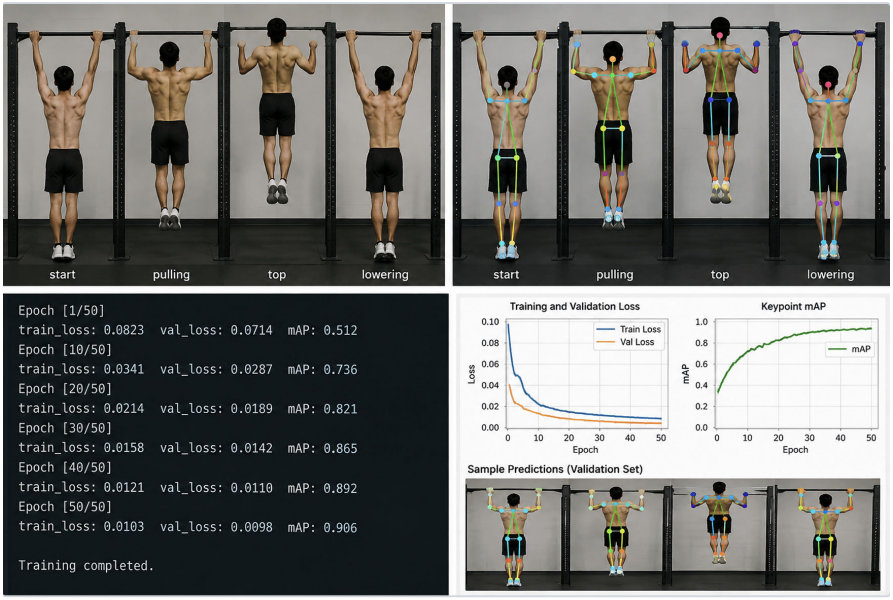
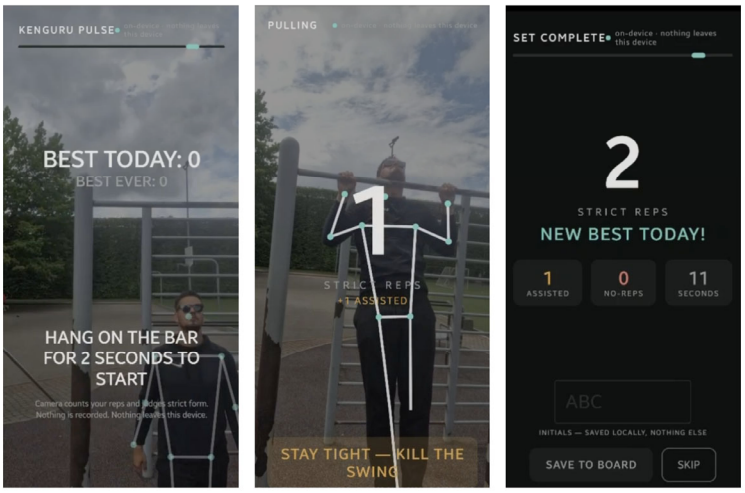


Figure 12. Training of the motion-analysis model: pull-up phases (start, pulling, top, lowering) without and with detected keypoints, training log, training and validation loss, keypoint mAP and sample predictions on the validation set.

Figure 13 shows the training module user interface during a set of pull-ups. The user starts a set by hanging on the bar for 2 s (Figure 13a). During the set, the skeleton overlay and repetition count are displayed; strict repetitions are counted separately from assisted repetitions and no-reps; and short cues address form errors such as body swing (Figure 13b). At the end of the set, the module summarises strict and assisted repetitions, no-reps and set duration (Figure 13c). All processing runs on the device, and it records and transmits no video.



(a) (b) (c)

Figure 13. User interface of the interactive training module: (**a**) start of a set; (**b**) repetition counting with a form cue; and (**c**) set summary.

3.3. Multi-System Integration

The integrated prototype's central element is the multi-hazard risk assessment executed by the central back-end processing unit. Rather than operating as isolated components, the subsystems exchange operational data to form a holistic safety and guidance matrix (as depicted in the overall system design in Figure 6). In the integrated design, one distribution cabinet, one UPS, one 4G/5G router and one on-site server serve all three subsystems. In contrast, separate deployments would each require their own power supply, backup, network connection and enclosure (Figure 2).

Table 1 summarises the interaction logic, visual indicators, and system responses. The staged scenarios (Figures 7–11) demonstrate interactions between visual detection and weather context, while interactions involving the heated bar follow the control logic described in Section 2.4.

Table 1. Integrated multi-hazard interaction matrix across prototype subsystems.

Primary Input & Environmental Triggers	Edge Processing & Real-Time AI Correlation	Automated Multi-System Output
Surveillance Camera—Optical precipitation (snowfall/rain) detected.	Recalculate surface friction risk; increase sensitivity to biomechanical instability.	Interactive display alerts user to slippery bar conditions; Luxriot VMS updates site risk level.
AI Motion Tracking—High-velocity uncontrolled trajectory or fall detected.	Spatial distress anomaly confirmed; user unresponsiveness measured.	The screen displays an emergency assistance prompt; an alert is sent to the person in charge through the Luxriot VMS.
Thermal Sensors—Bar temperature falls below +2 °C; ambient temperature <0 °C.	Sub-zero freezing risk confirmed on gripping surfaces.	The heating controller energises the heating cable; the interactive screen updates bar thermal readiness status.

4. Discussion

4.1. Power and Connectivity

The power design can be assessed against field evidence on standalone hybrid microgrids. According to Canziani et al. [41], solar-battery microgrids operating under real, measured field conditions can achieve supply reliability close to that of grid-connected installations, provided that battery capacity and photovoltaic sizing are matched to the site's seasonal irradiance profile; winter periods of reduced solar yield remain the principal risk window for autonomous operation, which is precisely why the UPS and 370 W LONGi array were retained as complementary, rather than sole, power sources in the present design. As Car et al. [34] explain, 5G-enabled edge architectures are expected to sustain telemetry latencies compatible with time-critical public-safety applications, which supports the use of a single industrial 4G/5G router for all subsystems. Taken together, these findings suggest that a single, consolidated power-and-connectivity backbone can substitute for the multiple redundant supplies typically required by fragmented smart outdoor infrastructures [38], without compromising the responsiveness needed for safety-critical alerts.

4.2. Surveillance and Incident Detection

The surveillance module's false-alarm suppression aligns with the broader literature on edge-based video anomaly detection. As explained by Patrikar and Parate [42] in their review of anomaly detection using edge computing in video surveillance, performing inference locally on the camera or an on-site server, rather than routing raw video to a remote cloud service, shortens detection latency and reduces the rate of spurious alerts caused by transmission artefacts and background motion; this supports the choice of on-site processing in the Luxriot VMS to keep alert dispatch within the 2 s design target and to limit false alarms. Sultani et al. [22] and Duong et al. [24] similarly reported that convolutional architectures trained to distinguish genuine human activity from environmental noise—wind, shadows, precipitation—substantially outperform simple motion-triggered alarms in outdoor public settings, supporting the design choice to fuse visual anomaly detection with weather-derived context rather than relying on visual cues alone.

4.3. Motion Analysis

The expected accuracy of the pose-estimation engine can be judged from recent independent benchmarking of markerless motion-capture systems. According to Edriss et al. [43], monocular RGB pose-estimation frameworks like those underlying commercial pose engines can approach the accuracy of laboratory-grade, marker-based systems for the sagittal-plane movements typical of callisthenics exercise. However, accuracy for out-of-plane or self-occluded joints remains comparatively lower—a limitation consistent with the present study's focus on frontal pull-up and dip-type movements. Cronin et al. [44] found that markerless pose analysis can perform reliably outside controlled laboratory conditions, against an unmodified real-world background, a finding directly relevant to the outdoor, unmarked field deployment evaluated here. As explained by Wade et al. [25] and O'Reilly et al. [29], removing the need for wearable sensors is a key precondition for safe unsupervised public use, since instrumentation cannot be assumed to be available or correctly worn by casual users; the system's reliance on a single fixed camera therefore represents a practical, and not merely technical, advantage over sensor-based alternatives for open-access municipal facilities.

The pose model processes the camera stream frame by frame on the edge device. Pose engines of this class run at more than 30 frames per second [26], keeping feedback delay within the range required for real-time user interaction.

Joint angle measurements across dynamic upper-body movements (e.g., elbow flexion/extension and shoulder abduction during pull-ups) are computed from the normalised keypoints. For monocular markerless systems, differences of 2.6–11° from marker-based reference systems have been reported [25], with smaller errors in the sagittal plane.

4.4. Heated Grip Zone

The heated grip zone can be assessed against two bodies of literature: anti-icing surface engineering and cold-contact injury thresholds. As Wang et al. [45] explain, self-regulating electrothermal surfaces that combine a positive-temperature-coefficient response with closed-loop control can suppress ice accretion on metallic substrates while avoiding the overheating risk associated with fixed-power heating elements, which is the operating principle of the self-regulating cable used in the prototype. Findings from full-scale resistive-heating deployments in transport infrastructure, such as the electrically conductive concrete pavement trialled by Malakooti et al. [46], likewise confirm that surface-temperature-based control, rather than ambient air-temperature thresholds alone, is required to reliably maintain above-freezing conditions across variable winter weather, supporting the decision to place thermal sensors directly on the bar surface rather than in the surrounding air. From a user-safety perspective, limit values for gripping cold steel and aluminium surfaces were derived so that skin-contact temperature does not fall below 15 °C [47]. A grip surface kept at +5 °C to +10 °C stays ice-free and above the freezing point of skin, although users will still feel cold during long grips; eliminating the cold sensation would require substantially higher heating power and energy use [30].

4.5. Integration and Limitations

Taken together, the multi-hazard interaction results support the central premise of this study: that consolidating surveillance, biomechanical monitoring, and thermal management onto a shared processing and power backbone can overcome the fragmentation identified as a key limitation of existing smart outdoor workout equipment. As explained by Muradoğlu et al. [35], integrated multi-sensor street infrastructure typically struggles to balance energy efficiency against multi-task computational load, since each subsystem is conventionally designed, procured, and powered independently; the prototype's single back-end fusion engine addresses this gap directly by correlating precipitation, motion, and thermal data within one risk-assessment pipeline instead of three disconnected ones. This is consistent with the efficiency gains reported by Huang et al. [38] for edge-computed infrastructure that shares compute and communication resources across functions and mirrors the efficiency rationale documented for the platform's own component integration. Nevertheless, the present evaluation was conducted on a single prototype installation, and, as is typical for early-stage climate-resilient infrastructure studies, longer-term, multi-site deployment across full seasonal cycles and sustained public use will be required to confirm that the detection performance and the expected thermal and energy performance hold beyond the conditions tested here.

5. Conclusions

This study presents the design and partial evaluation of an integrated, climate-resilient outdoor workout complex prototype that addresses the operational and safety limitations of traditional public fitness installations. By consolidating AI-driven security surveillance, markerless biomechanical feedback, active structural heating, and a shared power supply onto a single shared-infrastructure asset, the system removes the duplicated hardware and structural clutter characteristic of fragmented smart outdoor workout equipment. The following conclusions can be drawn:

- The grid-connected power architecture, with UPS backup and a 370 W solar panel, supplies all subsystems from one enclosure, and a single industrial 4G/5G router carries data from every subsystem, so power conversion, backup, and connectivity are not duplicated for each function.
- The surveillance subsystem, based on ColorVu cameras rated for full-colour imaging down to 0.0005 lux and on-site processing in the Luxriot VMS, recognised falls, loss of grip, slipping and prolonged immobility in staged outdoor scenarios and generated structured alerts for the person in charge, with a design target of 2 s from detection to notification.
- The monocular motion-analysis model, trained on participants with different body proportions and exercise techniques, normalises body keypoints, tracks the full exercise cycle, and counts repetitions; on the validation set, its keypoint mAP reached 0.906 after 50 training epochs. The system flags incorrectly executed repetitions and delivers real-time posture corrections on an interactive display while processing video exclusively in RAM to ensure user privacy.
- The heated grip zone uses a self-regulating heating cable that limits its own output as it warms and is switched by a surface temperature controller. At the same time, redundant sensors report bar temperature to the back end. Keeping the grip surface above 0 °C addresses both friction loss from ice and the risk of cold-contact injury identified in Section 1.
- A central back-end engine enabled multi-modal data fusion across all hardware modules. By correlating real-time optical precipitation detection (snow and rain) with user exercise mechanics, the central system dynamically adjusted safety risk thresholds and delivered automated, condition-specific hazard warnings.

The results indicate that unifying computational, sensing and thermal subsystems on a single structural asset is technically feasible for municipal sports facilities. By transforming passive workout equipment into interactive, year-round environments, this multifunctional architecture effectively addresses key barriers to winter utilisation, user injury risks, and unmonitored safety vulnerabilities in public spaces.

Based on these results, the following is recommended when smart functions are added to outdoor workout equipment: video should be processed on site without identity or facial recognition, and alerts should be verified by a person in charge before any response; heated grips should be controlled by sensors on the bar surface rather than by air temperature; and the power supply, backup, network connection and enclosure should be shared by all subsystems to avoid duplicated hardware.

Future research will quantify detection accuracy, pose-estimation accuracy and thermal and energy performance in extended multi-season field deployments and analyse long-term physical weathering, component durability, and maintenance cycles under continuous outdoor exposure. Further refinement of the computer vision algorithms to support simultaneous multi-user pose estimation and optimisation of the solar supply will enhance deployment flexibility in power-constrained urban and rural health parks.

Author Contributions: Conceptualisation, P.P.A. and M.S.; methodology, P.P.A., M.S. and A.I.; validation, M.S. and A.I.; formal analysis, P.P.A. and A.I.; investigation, P.P.A. and A.I.; resources, M.S.; data curation, P.P.A. and A.I.; writing—original draft preparation, P.P.A. and A.I.; writing—review and editing, P.P.A., M.S. and A.I.; visualisation, P.P.A.; supervision, M.S.; project administration, M.S.; funding acquisition, M.S. All authors have read and agreed to the published version of the manuscript.

Funding: This study was part of research project No. D. "1.6 Development of digital tools and safety systems for outdoor workout equipment", which was carried out under project No.

2.2.1.3.i.0/1/24/A/CFLA/007 'AMEMIL centre of excellence Support for the Development of Digital Products', with support from the European Union's Recovery and Resilience Facility.

Institutional Review Board Statement: Ethical review and approval were not required for this study in accordance with national legislation. In Latvia, an ethics committee opinion is required for clinical trials of medicinal products (Cabinet Regulation No. 192 of 26 March 2024), clinical investigations of medical devices (Cabinet Regulation No. 455 of 15 August 2023) and research using biobank samples (Biobank Law of 14 May 2026). This study was a non-interventional engineering evaluation of an outdoor workout prototype with adult volunteers; it did not involve medicinal products, medical devices, biological samples or health data. The only person shown in the figures is an author of this study.

Informed Consent Statement: Informed consent was obtained from all subjects involved in the study.

Data Availability Statement: The data presented in this study are available on reasonable request from the corresponding author. The data are not publicly available because they contain video recordings of participants.

Conflicts of Interest: Author Maris Slezins was employed by Ltd. Kenguru Pro, and Author Aleksandrs Ivasko was employed by Ltd. Aimconcept. The remaining author declares that the research was conducted without any commercial or financial relationships that could be construed as a potential conflict of interest.

Appendix A

Video Camera Pole

Figure A1 shows the layout of the video camera pole, the distribution cabinet and the underground cable route between them.

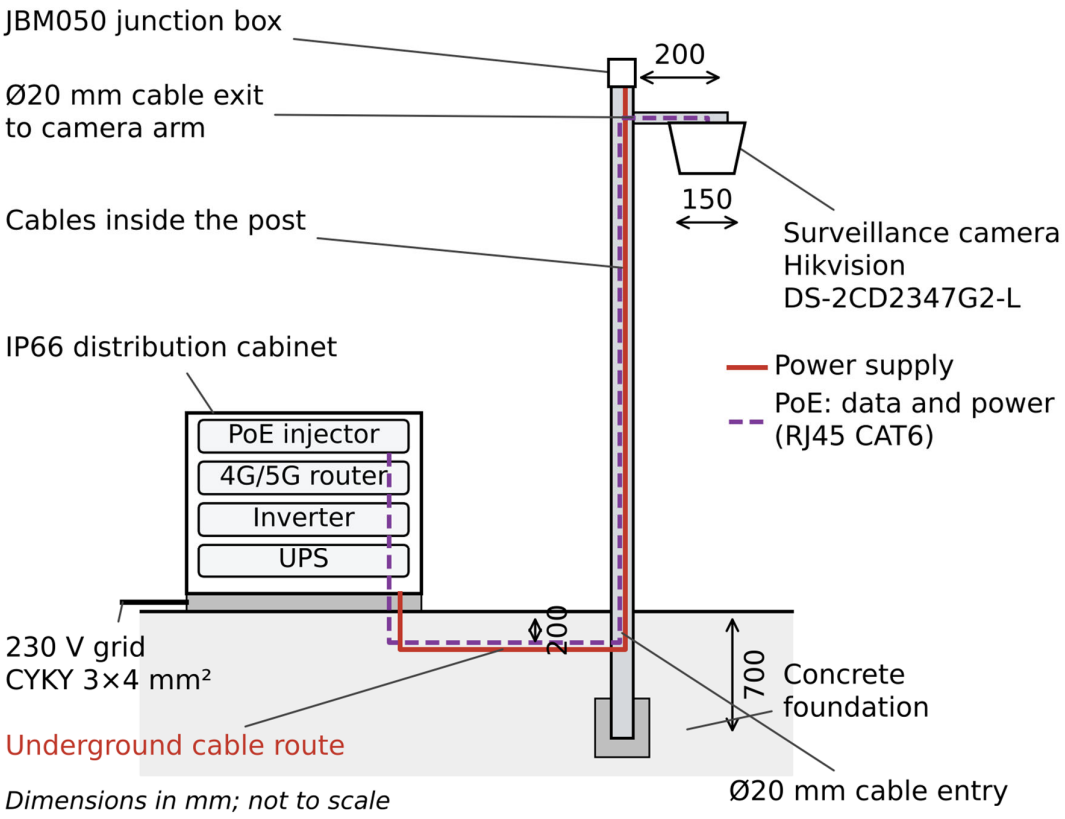


Figure A1. Layout of the video camera pole and its power and data connections (dimensions in mm, not to scale).

References

1. Bull, F.C.; Al-Ansari, S.S.; Biddle, S.; Borodulin, K.; Buman, M.P.; Cardon, G.; Carty, C.; Chaput, J.-P.; Chastin, S.; Chou, R.; et al. World Health Organization 2020 Guidelines on Physical Activity and Sedentary Behaviour. *Br. J. Sports Med.* **2020**, *54*, 1451–1462. https://doi.org/10.1136/bjsports-2020-102955.
2. Thompson, W.R. Worldwide Survey of Fitness Trends for 2021. *ACSMs Health Fit. J.* **2021**, *25*, 10–19. https://doi.org/10.1249/FIT.0000000000000631.
3. Cohen, D.A.; Han, B.; Nagel, C.J.; Harnik, P.; McKenzie, T.L.; Evenson, K.R.; Marsh, T.; Williamson, S.; Vaughan, C.; Katta, S. The First National Study of Neighborhood Parks: Implications for Physical Activity. *Am. J. Prev. Med.* **2016**, *51*, 419–426. https://doi.org/10.1016/j.amepre.2016.03.021.
4. Veitch, J.; Rivera, E.; Loh, V.; Paudel, C.; Biggs, N.; Deforche, B.; Timperio, A. Examining Park Features that Encourage Physical Activity and Social Interaction among Adults. *Health Promot. Int.* **2025**, *40*, daaf063. https://doi.org/10.1093/HEAPRO/DAAF063.
5. Sami, M.; Smith, M.; Ogunseitan, O.A. Changes in Physical Activity After Installation of a Fitness Zone in a Community Park. *Prev. Chronic Dis.* **2018**, *15*, 170560. https://doi.org/10.5888/PCD15.170560.
6. Chow, H.W.; Mowen, A.J.; Wu, G.L. Who Is Using Outdoor Fitness Equipment and How? The Case of Xihu Park. *Int. J. Environ. Res. Public Health* **2017**, *14*, 448. https://doi.org/10.3390/IJERPH14040448.
7. Sami, M.; Macridis, S.; Ogunseitan, O.A. Evaluating Actual Use of Outdoor Exercise Equipment in a Community Park in Southern California through Video-Captured Behavioral Assessment. *Discov. Public Health* **2025**, *22*, 598. https://doi.org/10.1186/S12982-025-01002-W.
8. Reuß, K.; Huth, C. Are Our Cities Falling behind? A German Perspective on the Supply for Year-Round Green Exercise. *Front. Sports Act. Living* **2025**, *7*, 1598959. https://doi.org/10.3389/FSPOR.2025.1598959.
9. Bergman, T.L.; Lavine, A.S.; Incropera, F.P.; DeWitt, D.P. *Fundamentals of Heat and Mass Transfer*, 8th ed.; John Wiley & Sons: Hoboken, NJ, USA, 2018; 992p.
10. Kietzig, A.M.; Hatzikiriakos, S.G.; Englezos, P. Ice Friction: The Effects of Surface Roughness, Structure, and Hydrophobicity. *J. Appl. Phys.* **2009**, *106*, 024303. https://doi.org/10.1063/1.3173346.
11. Ramadan, M.Z. The Effects of Industrial Protective Gloves and Hand Skin Temperatures on Hand Grip Strength and Discomfort Rating. *Int. J. Environ. Res. Public Health* **2017**, *14*, 1506. https://doi.org/10.3390/IJERPH14121506.
12. Ngo, J.K.; Solis-Urra, P.; Sanchez-Martinez, J. Injury Profile Among Street Workout Practitioners. *Orthop. J. Sports Med.* **2021**, *9*, 2325967121990926. https://doi.org/10.1177/2325967121990926.
13. Yadav, N.; Sharma, P. The Science of Calisthenics: Injury Epidemiology in Street Workout. *Indian J. YOGA Exerc. Sport Sci. Phys. Educ.* **2025**, *10*, 58–64. https://doi.org/10.58914/IJYESSPE.2025-10.2.10.
14. Gu, F.; Chung, M.H.; Chignell, M.; Valaee, S.; Zhou, B.; Liu, X. A Survey on Deep Learning for Human Activity Recognition. *ACM Comput. Surv.* **2022**, *54*, 177. https://doi.org/10.1145/3472290.
15. *EN 16630:2015*; Outdoor Fitness Equipment Safety Standards. European Committee for Standartization: Brussels, Belgium, 2015.
16. *BS EN 1177:2018*; Impact Attenuating Playground Surfacing—Methods of Test for Determination of Impact Attenuation. The British Standard: London, UK, 2019.
17. *ISO 13732-3:2005*; Ergonomics of the Thermal Environment-Methods for the Assessment of Human Responses to Contact with Surfaces Part 3: Cold Surfaces. The British Standard: London, UK, 2008.
18. European Parliament. *Regulation—2016/679*; 2016. Available online: https://eur-lex.europa.eu/eli/reg/2016/679/oj/eng (accessed on 9 November 2026).
19. European Parliament. *Regulation—EU—2024/1689*; 2024. Available online: https://eur-lex.europa.eu/eli/reg/2024/1689/oj/eng (accessed on 9 November 2026).
20. Hikvision USA ColorVu—Low-Light Imaging. Available online: https://www.hikvision.com/us-en/core-technologies/low-light-imaging/colorvu/ (accessed on 22 September 2026).
21. Hikvision Europe Pro Series with ColorVu 3.0—Network Cameras. Available online: https://www.hikvision.com/europe/products/IP-Products/Network-Cameras/colorvu-products/?category=Network+Products&subCategory=Network+Cameras&series=Pro+Series+%28EasyIP%29&checkedSubSeries=NONE (accessed on 22 September 2026).
22. Sultani, W.; Chen, C.; Shah, M. Real-World Anomaly Detection in Surveillance Videos. In Proceedings of the IEEE/CVF Conference on Computer Vision and Pattern Recognition (CVPR), Salt Lake City, UT, USA, 18–23 June 2018.

23. Abdalla, M.; Javed, S.; Al Radi, M.; Ulhaq, A.; Werghi, N. Video Anomaly Detection in 10 Years: A Survey and Outlook. *Neural Comput. Appl.* **2024**, *37*, 26321–26364. https://doi.org/10.1007/s00521-025-11659-8.
24. Duong, H.T.; Le, V.T.; Hoang, V.T. Deep Learning-Based Anomaly Detection in Video Surveillance: A Survey. *Sensors* **2023**, *23*, 5024. https://doi.org/10.3390/S23115024.
25. Wade, L.; Needham, L.; McGuigan, P.; Bilzon, J. Applications and Limitations of Current Markerless Motion Capture Methods for Clinical Gait Biomechanics. *PeerJ* **2022**, *10*, e12995. https://doi.org/10.7717/PEERJ.12995.
26. Bazarevsky, V.; Grishchenk, I. On-Device, Real-Time Body Pose Tracking with MediaPipe BlazePose. 2020. Available online: https://research.google/blog/on-device-real-time-body-pose-tracking-with-mediapipe-blazepose/ (accessed on 9 November 2026).
27. Lugaresi, C.; Tang, J.; Nash, H.; Mcclanahan, C.; Uboweja, E.; Hays, M.; Zhang, F.; Chang, C.-L.; Yong, M.G.; Lee, J.; et al. MediaPipe: A Framework for Building Perception Pipelines. *Distrib. Parallel Clust. Comput.* **2019**. Available online: https://arxiv.org/abs/1906.08172 (accessed on 9 November 2026).
28. Sinclair, A.; Kautai, K.; Shahamiri, S.R. On-Device Real-Time Smartphone-Based Automated Exercise Repetition Counting System. 2023. Available online: https://arxiv.org/abs/2308.02420 (accessed on 9 November 2026).
29. O'Reilly, M.; Caulfield, B.; Ward, T.; Johnston, W.; Doherty, C. Wearable Inertial Sensor Systems for Lower Limb Exercise Detection and Evaluation: A Systematic Review. *Sports Med.* **2018**, *48*, 1221–1246. https://doi.org/10.1007/S40279-018-0878-4.
30. Shchegolkov, A.V.; Shchegolkov, A.V.; Kaminskii, V.V.; Chumak, M.A. Smart Polymer Composites for Electrical Heating: A Review. *J. Compos. Sci.* **2024**, *8*, 522. https://doi.org/10.3390/jcs8120522.
31. Guo, X.; Yang, Q.; Zheng, H.; Dong, W. Optimization of Power Distribution for Electrothermal Anti-Icing Systems by Differential Evolution Algorithm. *Appl. Therm. Eng.* **2023**, *221*, 119875. https://doi.org/10.1016/J.APPLTHERMALENG.2022.119875.
32. Minh, Q.N.; Nguyen, V.H.; Quy, V.K.; Ngoc, L.A.; Chehri, A.; Jeon, G. Edge Computing for IoT-Enabled Smart Grid: The Future of Energy. *Energies* **2022**, *15*, 6140. https://doi.org/10.3390/EN15176140.
33. Teltonika RUTX50 Industrial 5G Router|Teltonika. Available online: https://www.teltonika-networks.com/products/routers/rutx50 (accessed on 22 September 2026).
34. Car, T.; Pilepić Stifanich, L.; Kovačić, N. The Role of 5G and IoT in Smart Cities. *Entren. Enterp. Res. Innov.* **2022**, *8*, 377–389. https://doi.org/10.54820/ENTRENOVA-2022-0032.
35. Muradoğlu, S.N.; Deniz, D. Smart Energy Applications and Integration of Urban Furniture into Smart Systems in Cities. *Int. J. Energy Prod. Manag.* **2022**, *7*, 127–139. https://doi.org/10.2495/EQ-V7-N2-127-139.
36. Luder, V.; Magno, M. Self-Sustaining Multi-Sensor LoRa-Based Activity Monitoring for Community Workout Parks. In Proceedings of the IEEE Sensors Applications Symposium, SAS, Newcastle, UK, 8–10 July 2025. https://doi.org/10.1109/SAS65169.2025.11105143.
37. Cocconcelli, F.; Matrella, G.; Mora, N.; Casu, I.; Vargas Godoy, D.A.; Ciampolini, P. IoT Smart Flooring Supporting Active and Healthy Lifestyles. *Sensors* **2023**, *23*, 3162. https://doi.org/10.3390/S23063162.
38. Huang, J.; Zhou, S.; Li, G.; Shen, Q. Real-Time Monitoring and Optimization Methods for User-Side Energy Management Based on Edge Computing. *Sci. Rep.* **2025**, *15*, 24890. https://doi.org/10.1038/S41598-025-07592-4.
39. BriskHeat Corporation Self-Regulating Heating Cable 8W 120V Fluoropolymer. Available online: https://www.briskheat.com/products/low-temperature-self-regulating-heating-cable-slcbl?srsltid=AYCX9vJ-OJF58GgBeRgnq68TJKS-XpWjgc2g4yN9crZpiuOggR4n5otjJ (accessed on 16 November 2026).
40. BriskHeat Corporation Digital Temperature Controller in NEMA 4X Enclosure. Available online: https://www.briskheat.com/products/tc4x-digital-temperature-controller-in-nema-4x-enclosure?srsltid=AYCX9vJ_LLZZSOjjr9XL04S1suvilOIB4kUd3xyOya1G5SEWu115nV9Y (accessed on 16 November 2026).
41. Canziani, F.; Vargas, R.; Castilla, M.; Miret, J. Reliability and Energy Costs Analysis of a Rural Hybrid Microgrid Using Measured Data and Battery Dynamics: A Case Study in the Coast of Perú. *Energies* **2021**, *14*, 6396. https://doi.org/10.3390/EN14196396.
42. Patrikar, D.R.; Parate, M.R. Anomaly Detection Using Edge Computing in Video Surveillance System: Review. *Int. J. Multimed. Inf. Retr.* **2022**, *11*, 85–110. https://doi.org/10.1007/S13735-022-00227-8.
43. Edriss, S.; Romagnoli, C.; Caprioli, L.; Bonaiuto, V.; Padua, E.; Annino, G. Commercial Vision Sensors and AI-Based Pose Estimation Frameworks for Markerless Motion Analysis in Sports and Exercises: A Mini Review. *Front. Physiol.* **2025**, *16*, 1649330. https://doi.org/10.3389/FPHYS.2025.1649330.
44. Cronin, N.J.; Walker, J.; Tucker, C.B.; Nicholson, G.; Cooke, M.; Merlino, S.; Bissas, A. Feasibility of OpenPose Markerless Motion Analysis in a Real Athletics Competition. *Front. Sports Act. Living* **2024**, *5*, 1298003. https://doi.org/10.3389/FSPOR.2023.1298003.

45. Wang, Z.; Zhu, Y.; Liu, X.; Zhao, Z.; Chen, J.; Jing, X.; Chen, H. Temperature Self-Regulating Electrothermal Pseudo-Slippery Surface for Anti-Icing. *Chem. Eng. J.* **2021**, *422*, 130110. https://doi.org/10.1016/J.CEJ.2021.130110.
46. Malakooti, A.; Sadati, S.; Ceylan, H.; Kim, S.; Cetin, K.S.; Taylor, P.C.; Mina, M.; Cetin, B.; Theh, W.S. *Self-Heating Electrically Conductive Concrete Demonstration Project*; Iowa State University: Ames, IA, USA, 2021.
47. Malchaire, J.; Kampmann, B.; Mehnert, P.; Gebhardt, H.; Piette, A.; Havenith, G.; Holmér, I.; Parsons, K.; Alfano, G.; Griefahn, B. Assessment of the Risk of Heat Disorders Encountered during Work in Hot Conditions. *Int. Arch. Occup. Environ. Health* **2002**, *75*, 153–162. https://doi.org/10.1007/S004200100287.

Disclaimer/Publisher's Note: The statements, opinions and data contained in all publications are solely those of the individual author(s) and contributor(s) and not of MDPI and/or the editor(s). MDPI and/or the editor(s) disclaim responsibility for any injury to people or property resulting from any ideas, methods, instructions or products referred to in the content.